



HAL
open science

The use of a Phenomenological, multizone combustion Model to investigate emissions from Marine diesel engines

Xavier Tauzia, Jean-François Hétet, Pascal Chessé, Bahadir Inozu, Philippe Roy

► To cite this version:

Xavier Tauzia, Jean-François Hétet, Pascal Chessé, Bahadir Inozu, Philippe Roy. The use of a Phenomenological, multizone combustion Model to investigate emissions from Marine diesel engines. Fall Technical Conference of the Internal Combustion Engine Division of the ASME, 2000, Peoria, United States. hal-01155851

HAL Id: hal-01155851

<https://hal.science/hal-01155851>

Submitted on 6 Feb 2019

HAL is a multi-disciplinary open access archive for the deposit and dissemination of scientific research documents, whether they are published or not. The documents may come from teaching and research institutions in France or abroad, or from public or private research centers.

L'archive ouverte pluridisciplinaire **HAL**, est destinée au dépôt et à la diffusion de documents scientifiques de niveau recherche, publiés ou non, émanant des établissements d'enseignement et de recherche français ou étrangers, des laboratoires publics ou privés.

THE USE OF A PHENOMENOLOGICAL, MULTIZONE COMBUSTION MODEL TO INVESTIGATE EMISSIONS FROM MARINE DIESEL ENGINES

Xavier TAUZIA
Jean-François HETET
Pascal CHESSE

Laboratory of fluid mechanics - U.M.R. C.N.R.S. 6598
Ecole Centrale de Nantes
Nantes, FRANCE

Bahadir INOZU
Philippe ROY

School of Naval Architecture & Marine Engineering
University of New Orleans
New Orleans, Louisiana

ABSTRACT

During the past decade, large marine diesel engines have been the subject of increased rules and regulations aimed at reducing pollutant emissions, now critical in the design and operation of marine propulsion systems. This paper presents a phenomenological multi-zone combustion model designed to evaluate the efficiency of the various techniques used to reduce pollutant emissions. The model's validation was achieved by comparing simulated NOx concentrations and smoke opacities with experimental measurements. Subsequently, the code was used to evaluate the effect of four of the main pollution control techniques not only on pollutant emissions but also on the global engine performance and efficiency.

NOMENCLATURE

Variable	Unit	Description
\dot{H}_{air}	J/s	enthalpy of air entering a zone
\dot{H}_{fv}	J/s	enthalpy of fuel entering a zone
\dot{m}_{air}	kg/s	mass flow of air displaced inside a zone
\dot{m}_b	kg/s	mass flow of burnt gas
\dot{m}_{bc}	kg/s	combustion rate limit induced by chemical kinetics
\dot{m}_{bp}	kg/s	pre-mixed combustion rate
\dot{m}_{bd}	kg/s	diffusion combustion rate
\dot{m}_{bt}	kg/s	combustion rate limit induced by turbulent mixture
\dot{m}_l	kg/s	fuel mass flow in liquid state
\dot{m}_{fv}	kg/s	mass variation of vaporized fuel
\dot{m}_{inj}	kg/s	fuel mass flow injected in a zone

\dot{m}_{inj_tot}	kg/s	instantaneous injected fuel mass flow
\dot{m}_{sc}	kg/s	soot oxidation rate
\dot{m}_{sf}	kg/s	soot formation rate
\dot{m}_{vap}	kg/s	evaporation mass flow in a zone
\dot{m}_{xp}	kg/s	air/fuel mixture preparation rate
A_{sf}, A_{sc}	-	constants
C	-	concentration inside the spray
$C(C_m)$	-	maximum concentration inside the spray
$C_{l_{air}}$	-	air entrainment coefficient
$C_{d_{noz}}$	-	discharge coefficient at injector's nozzle
C_{st}	-	stoichiometric fuel/air ratio
d_{noz}	m	orifice diameter
\dot{Q}_b	W	power generated by combustion
$\dot{Q}_w, \dot{Q}_{w_tot}$	W	total thermal loss at the cylinder wall for a zone
h_{air}	J/kg	specific enthalpy of incoming air
h_{fv}	J/kg	specific enthalpy of the fuel
K_{cpm}, K_{di}	-	constants
KTI	s ⁻¹	rate of turbulent mixing
m_a	kg	air mass in a zone
m_b	kg	mass of burnt fuel
MCR		Maximum Continuous Rating
m_{fuel_tot}	kg	total mass of injected fuel
m_{fv}	kg	mass of vaporized fuel
m_g	kg	mass of gas in a zone
m_{inj}	kg	mass of fuel injected in a zone
m_p	kg	mass of air/fuel mixture prepared but yet to be burnt
m_{sh}	kg	mass of soot in a zone
LHV	J/kg	lower calorific value
P_{cy}	Pa	cylinder pressure
R	J/mol/K	universal gas constant
Re	-	Reynolds in the cylinder
s	m	spray penetration in a zone
S_{cyl}	m ²	cylinder area during cycle

SMD	m	Sauter's mean diameter
S_{noz}	m^2	injector's sectional area
T	K	zone temperature
t	s	time
T_{cc}	K	constant
T_{cyl}	K	average temperature in the cylinder
t_{debinj}	s	injection timing
T_{di}, T_{pm}	K	constants
T_w	K	cylinder wall temperature
U (U_m)	m/s	maximum spray velocity
v	m/s	zone velocity
V_{cy}	m^3	cylinder volume as a function of time
vol	m^3	zone volume
vol _{air}	m^3	volume of fresh gas
ΔP_{noz}	Pa	inlet/outlet pressure difference at the injector's orifice
ρ_{cy}	kg/m^3	cylinder gas density
ρ_{fuel}	kg/m^3	fuel density
τ_{Bup}	s	duration of spray break-up
τ_{inf}	s	ignition delay
τ_{vap}	s	duration of evaporation

INTRODUCTION

Following years of discussions, the rules of the International Maritime Organization (IMO 1996) restricting the pollutant emissions of marine diesel engines are now applicable on an international basis. In addition, some local restrictions are even more stringent in sensitive areas such as the Baltic sea, California and ports. The violation of these restrictions may result in severe financial penalties. It has thus become critical to keep pollutant emissions under control while maintaining satisfactory levels of efficiency, performance and reliability.

Test bed measurements are usually tedious and expensive. As a result, the use of engine simulation codes is an attractive solution. The following two fundamental principles are being used by the vast majority of the currently available simulation codes (Heywood 1988):

- Computational Fluid Dynamics (CFD): such codes aim at solving the equation of Navier-Stokes inside a cylinder (Reitz et al. 1995). They allow a very precise description of physical processes; however, their implementation is quite tedious.
- Phenomenological models: such codes are based on semi empirical equations partially derived from experiments. They are somewhat dependent on test bed measurements.

The second approach has been selected for the study presented in this paper because it allows the simultaneous investigation of the effect of pollution control techniques and their influence on the global performance of the engine as well as its auxiliaries, such as the air charging system. The proposed solution consists of extending the SELENDIA simulation code that has been developed by the authors for a decade (Hétet et al. 1994, Hétet et al. 1999) by adding a multi-zone combustion model allowing the evaluation of NO_x and particulate emissions.

I. COMBUSTION MODEL AND EVALUATION OF POLLUTANT EMISSIONS

Since diesel combustion initiates from a fuel spray injected in the cylinder, the model is based on the division of a spray into a number of zones with their own thermodynamic characteristics, including temperature and air/fuel ratio. During the length of the injection process, the fuel spray is divided into m segments, with each segment being divided itself into n zones, from the spray axis to its outer envelop as shown in Figure 1. As a result, the spray is divided into (m × n) zones with an additional zone for the fresh inlet air that will be progressively displaced by the spray. Each zone is characterized by its own set of equations providing its temperature and local fuel/air ratio and eventually the quantity of pollutants being formed. The modeled injector includes 9 nozzles; however, only one spray generated by one nozzle is actually modeled since the remaining sprays can be acquired using symmetry.

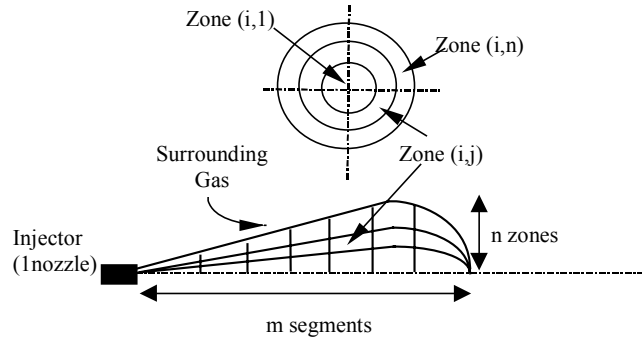


Figure 1. Schematic of the Multi-zone Diesel Combustion Model

Since each spray is assumed to be symmetric around its axis, the zones are actually ring-shaped, with the number 1 zone located on the axis and the number n zone located at the outer limit of the spray.

Injection

The instantaneous injection flow is evaluated using the following equation derived from Bernoulli:

$$\dot{m}_{inj_tot} = \rho_{fuel} S_{noz} C_{d_noz} \sqrt{2\Delta P_{noz} / \rho_{fuel}} \quad (1.)$$

The injection pressure and needle lift as a function of the crank angle are provided by experimental measurements. The discharge coefficient C_{d_noz} was obtained from the experiment.

Expansion of the fuel spray

Immediately following the injection, the spray preserves a compact shape for a limited time and then is subsequently atomized into small liquid drops. The duration of the atomization process is evaluated using an empirical formulation provided by Hiroyasu et al. (1983) and also used by Bazari (1993):

$$\tau_{bup} = 28.65 d_{noz} \rho_{fuel} / \sqrt{\rho_{cy} \Delta P_{noz}} \quad (2.)$$

In the mean time, the velocity is assumed to remain unchanged and equal to its value at the injector outlet. Then, the following formulation provided by Hiroyasu et al. (1983) for the penetration of a free turbulent spray is applied:

$$s = 2.95(\Delta P_{noz}/\rho_{cy})^{0.25} \sqrt{d_{noz}t} \quad (3.)$$

The velocity on the jet axis is obtained by differentiation of the equation used for the spray penetration. Subsequently, the velocity of the various zones is calculated using the standard techniques predicting an exponential decrease from the outer limit to the center:

$$v(i,j) = v(i,1) \exp\left[-8.557 \times 10^{-3} \left(9 \times \frac{j-1}{n-1}\right)^2\right] \quad (4.)$$

The above equation is derived from the one used by Hiroyasu, rendered dimensionless to allow a variable number of zones.

The velocity of each zone at the base of the spray impact on the cylinder wall is assumed to be parallel to the wall. To account for the speed reduction generated by the impact, the $t^{0.5}$ term in equation 3 characterizing the spray penetration was replaced with $t^{0.25}$ (Nishida et al. 1989).

The mathematical formulation describing the air entrainment by the spray is based on the experimental observations published by Haupais (1982). These observations showed a decrease of the fuel/air ratio that is proportional to $1/x$ along the spray axis. Subsequently, the air entrainment by the spray is given by the following equation:

$$\begin{aligned} \dot{m}_{air}(i,1) = & \frac{m_{inj}(i,1)}{Cl_{air}} \times \frac{1}{d_{noz} \sqrt{\rho_{fuel}/\rho_{cy}}} \times \dot{s}(i,1) \\ & + \frac{1}{Cl_{air}} \times \dot{m}_{inj}(i,1) \frac{s(i,1)}{d_{noz} \sqrt{\rho_{fuel}/\rho_{cy}}} \end{aligned} \quad (5.)$$

At the end of the spray impact on the cylinder wall, the entrainment coefficient Cl_{air} is divided by 1.5 to take into consideration the reduction in momentum associated with this phase (Hiroyasu et al. 1983). The air entrainment in any zone is calculated to fit the concentration profile of an established spray using the following equation:

$$\frac{C}{C_m} = \left(\frac{U}{U_m}\right)^{\frac{1}{2}} \quad (6.)$$

Finally, the following formula is obtained:

$$\dot{m}_{air}(i,j) = \frac{2j-1}{\sqrt{\exp\left[-8.557 \times 10^{-3} \times \left(\frac{9(j-1)}{n-1}\right)^2\right]}} \times \dot{m}_{air}(i,1) \quad (7.)$$

Preparation of the fuel and combustion

The fuel evaporation is modeled assuming the formation of identical drops with a diameter equal to the average Sauter's diameter, obtained as a function of the various injection variables using the formula provided by Hiroyasu et al. (1983):

$$SMD = 23.9 \times 10^{-6} (\Delta P_{noz} \times 10^{-5})^{-0.135} \rho_{cy}^{0.121} (m_{fuel_tot} \times 10^{-6})^{0.131} \quad (8.)$$

From the beginning of the injection process in a segment, the evaporation kinetic in a drop is evaluated using the method published by Lefevbre (1988). It includes an initial period during which the drop is heated followed by a steady state. The fuel

characteristics, the ambient pressure and temperature and the velocity of the drop in the surrounding air are parameters of the model. When the duration of the evaporation process is known, the mass of fuel vaporized is calculated by introducing a delay in the injected mass profile using the following equation:

$$\dot{m}_{vap}(i,j)(t) = \dot{m}_{inj}(i,j)(t - \tau_{vap}(i)) \quad (9.)$$

Each of the three combustion phases is modeled separately. A mixing of air and vaporized fuel occurs during the ignition delay. The mixing rate \dot{m}_{xp} is evaluated using the concentration of each constituent and the characteristics of the turbulence:

$$\dot{m}_{xp} = KTI \times \text{Min}\left(\frac{m_a}{C_{st}}, m_{fv}\right) (C_{st} + 1) \quad (10.)$$

The ignition occurs as soon as the following requirement is fulfilled:

$$\left(\int_{t_{debinj}}^t \frac{1}{\tau_{inf}} dt\right) \geq 1 \quad (11.)$$

where $\tau_{inf}(i,j) = K_{di} \times P_{cy}^{-2.5} \times \exp\left(\frac{T_{di}}{T(i,j)}\right)$ (12.)

The values of K_{di} and T_{di} , respectively 0.01 and 4500, were evaluated from measured ignition delays. The mixture prepared during the ignition delay subsequently burns while following a simple kinetic reaction of the Arrhenius type:

$$\dot{m}_{bp} = k_{cpm} \times m_p \times \exp\left(-\frac{T_{pm}}{T}\right) \quad (13.)$$

In addition, as soon as the ignition occurs, the air and fuel that were yet to be prepared start burning as their turbulent mixing progresses, leading to the diffusion phase of the combustion. The combustion rate is provided by the following equation:

$$\dot{m}_{bt} = KTI \times \text{Min}\left(\frac{m_a}{C_{st}}, m_{fv}\right) (C_{st} + 1) \quad (14.)$$

In an attempt to understand the influence of temperature on combustion rate, which might be predominant for low temperatures, a combustion rate related to chemical kinetics is also defined from a formulation proposed by Nishida et al. (1989):

$$\dot{m}_{bc} = K_{cc} \times \left(\frac{m_g}{vol}\right)^2 \times \left(\frac{m_a}{m_g}\right)^5 \times \left(\frac{m_{fv}}{m_g}\right) \times \exp\left(-\frac{T_{cc}}{T}\right) \times (C_{st} + 1) \quad (15.)$$

The values of K_{cc} and T_{cc} are those proposed by Nishida, respectively 5×10^{10} and 12000. T_{pm} is equal to T_{cc} and the value of k_{cpm} was fitted based on experimental in-cylinder pressure profiles. Finally, the combustion rate is provided by the following equation:

$$\dot{m}_{bd} = \text{Min}(\dot{m}_{bc}, \dot{m}_{bt}) \quad (16.)$$

The values of the mixing rate KTI and the coefficient Cl_{air} characterizing the air entrainment are hard to obtain directly. Since no experimental information on the internal processes occurring inside the cylinder is available, a parametric formulation of these coefficients was proposed as a function of the spray kinetic energy and the engine speed (Tauzia 1998), whose predominant roles were established by Smith et al. (1997).

Conservation Equations and Resolution

Each zone may contain some liquid fuel, vaporized fuel, air, mixture prepared during the ignition delay and ready to burn, and burnt gas as shown in Figure 2.

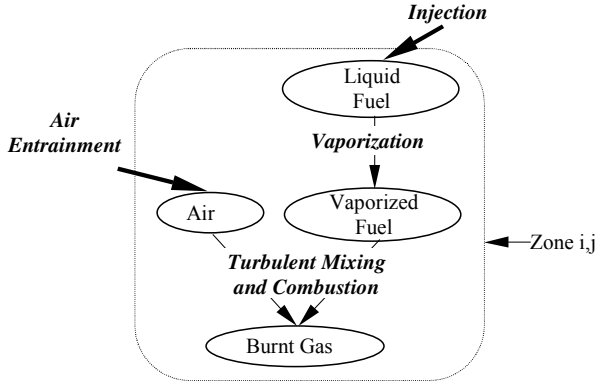


Figure 2. Summary of Mass Conservation for a Zone of the Spray

The mass conservation equations are the following:

$$\dot{m}_f = \dot{m}_{inj} - \dot{m}_{vap} \quad (17.)$$

$$\dot{m}_{fv} = \dot{m}_{vap} - \dot{m}_b \times \frac{1}{C_{st} + 1} \quad (18.)$$

$$\dot{m}_a = \dot{m}_{air} - \dot{m}_b \times \frac{C_{st}}{C_{st} + 1} \quad (19.)$$

$$\dot{m}_b = \dot{m}_{bp} + \dot{m}_{bd} \quad (20.)$$

The energy conservation includes the enthalpy of the air and fuel entering each zone, the heat released by the fuel combustion as well as the heat loss at the cylinder walls using the following formulation:

$$\dot{H}_{fv} = \dot{m}_{vap} \times h_{fv} \quad (21.)$$

$$\dot{H}_{air} = \dot{m}_{air} \times h_{air} \quad (22.)$$

$$\dot{Q}_b = \dot{m}_b \times LHV \quad (23.)$$

The global heat exchange at the cylinder walls are modeled using the equation of Annand (1963):

$$\dot{Q}_{w_tot} = K_{pp} \times Re^{0.7} \times (T_{cyl} - T_w) \times S_{cyl} \quad (24.)$$

The Reynolds number (Re) inside the cylinder is evaluated from the average piston velocity. The value of K_{pp} was obtained from the experiment. The combustion of each zone is expressed as a function of its mass and temperature difference with the cylinder wall using the following equation:

$$\dot{Q}_w = \dot{Q}_{w_tot} \left(\frac{m_g(T - T_w)}{\sum_{zones} m_g(T - T_w)} \right) \quad (25.)$$

The mass and energy transfers being known, the first law of thermodynamics can be applied to each zone to get access to its temperature. The pressure is assumed to be uniform inside the

cylinder. It is evaluated by using the ideal gas law and the following equation describing the volume conservation:

$$\sum Vol(i,j) + Vol_{air} = V_{cy} \quad (26.)$$

Formation of Pollutant Emissions

Pollutant emissions are estimated in each zone based on its temperature and local fuel/air ratio. They are subsequently added up to obtain the quantity of pollutants produced in the entire cylinder. The NO_x formation is evaluated using the model of Zeldovitch (Heywood 1988):



The equilibrium concentrations are calculated using the method provided by Olikara and Borman (Fergusson 1986). The following dual equation model provided by Hiroyasu (1983) is used for the soot formation:

$$\dot{m}_{sf} = A_{sf} m_{fv} P_{cy}^{0.5} \exp\left(-\frac{50000}{RT}\right) \quad (30.)$$

$$\dot{m}_{sc} = A_{sc} m_s P_{cy}^{0.8} \left(0.23 P_{cy} \frac{m_a}{m_g}\right) \exp\left(-\frac{56000}{RT}\right) \quad (31.)$$

The values of A_{sf} and A_{sc} were calculated to allow 10% of the fuel to take part in the soot formation. In addition, they were fitted with measured exhaust concentrations. The pollutant concentrations at the exhaust are calculated assuming that fresh air and burnt gas do not mix during the scavenge phase (Tauzia et al. 1997). The particle concentrations are converted into smoke opacity, or Bosh index, using an experimental equivalence.

2. MODEL VALIDATION

2.1 Test engines

Table 1 provides the main characteristics of the two test engines used for validation.

Table 1. Main characteristics of the test engines

Engine	A	B
type:	4 stroke	4 stroke
bore:	280 mm	400 mm
stroke:	290 mm	500 mm
rotation speed at MCR:	1050 rpm	550 rpm
BMEP at MCR:	21 bar	23 bar
power at MCR:	325 kW/cyl	615 kW/cyl
boost pressure at MCR:	3.7 bar	3.6 bar
turbocharging:	sequential	single-stage

Both engines are medium speed diesel engines used for marine propulsion and power generation, representative of two power ranges. Engine A is sequentially turbocharged (Hermann 1990). All experimental measurements were conducted by the engine manufacturer. They are not provided in this paper for confidentiality reasons.

2.2 Evaluation of the cylinder pressure

The comparison between experimental and calculated pressure profiles obtained with the multi-zone model shows a good agreement. Figure 3 shows the results obtained for engine A at high engine rpm and high load, high engine rpm and low load, low engine rpm and high load, and low engine rpm and low load, respectively. These various operating conditions allow a representative description of the complete engine operation range and their associated types of combustion (pre-mixed and diffusion). For all cases, the location on the time scale of the key pressure values, such as the combustive timing and the maximum cylinder pressure, is satisfactory since the maximum difference between measured and calculated data does not exceed one or two crank angles.

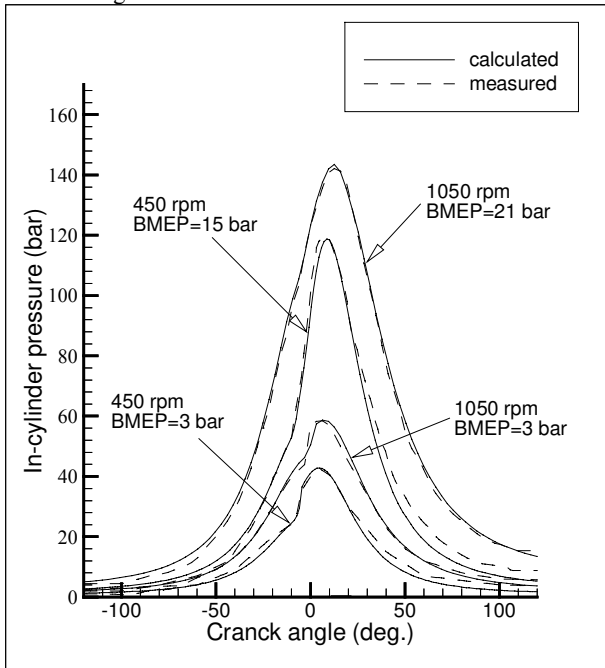


Figure 3. In-cylinder Pressure Variations during Combustion. Comparison between Calculations and Experiment – Engine A

Similar results were obtained for engine B as shown in Figure 4.

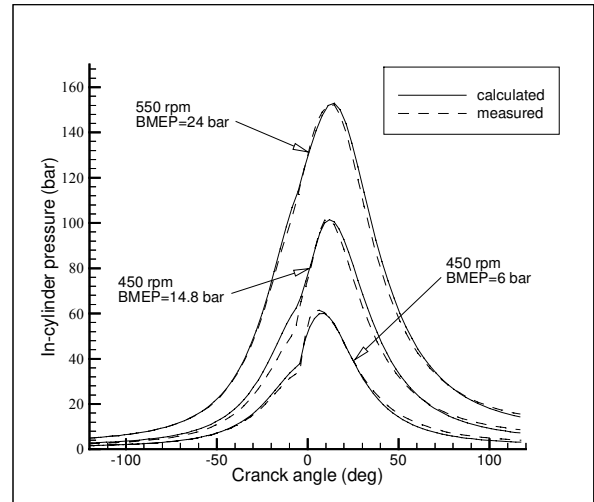


Figure 4. In-cylinder Pressure Variations during Combustion. Comparison between Calculations and Experiment – Engine B

2.3 Evaluation of pollutant emissions

Figures 5 and 6 show the absolute value of the relative difference between measured and computed NO_x emissions, i.e., $|\text{NO}_x_{\text{computed}} - \text{NO}_x_{\text{measured}}|$ divided by $\text{NO}_x_{\text{measured}}$, for the complete operation range of engine A and B. The difference is less than 20% on most of the operation range. This can be considered satisfactory, especially with respect to the uncertainty in experimental measurements that can be as high as 30% under certain operating conditions, especially low rpm or low load. Indeed, the evaluation of the general engine operation is achieved with a rather high degree of inexactitude due in part to the inaccuracy of the manufacturer's turbocharger maps in these areas of operation. This uncertainty is combined with the inexactitude inherent to the model.

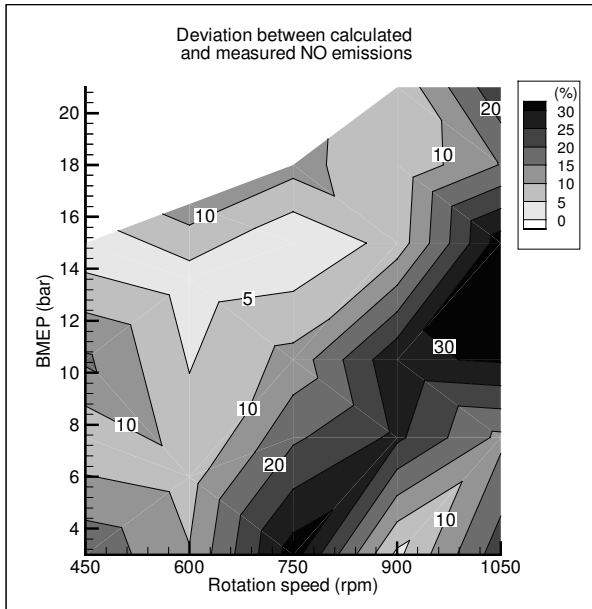


Figure 5. Difference between Measured and Simulated NOx Concentrations – Engine A

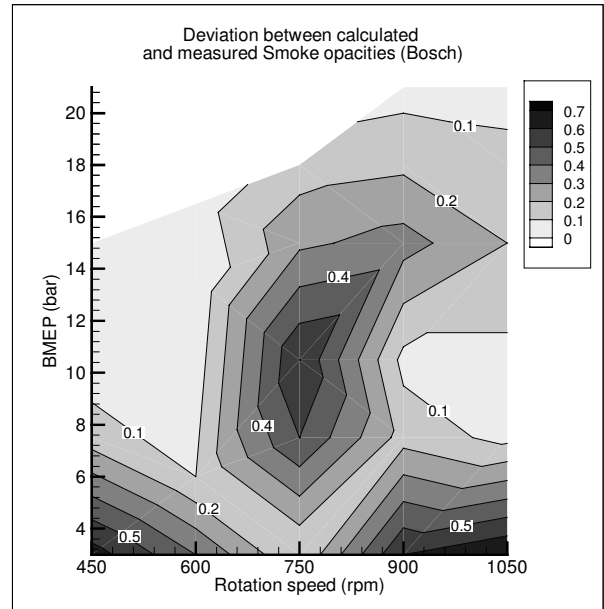


Figure 7. Difference between Measured and Simulated Smoke Opacities – Engine A

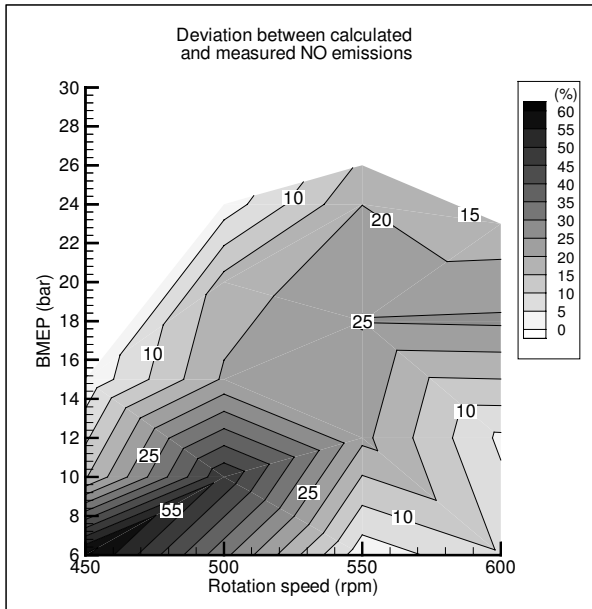


Figure 6. Difference between Measured and Simulated NOx Concentrations – Engine B

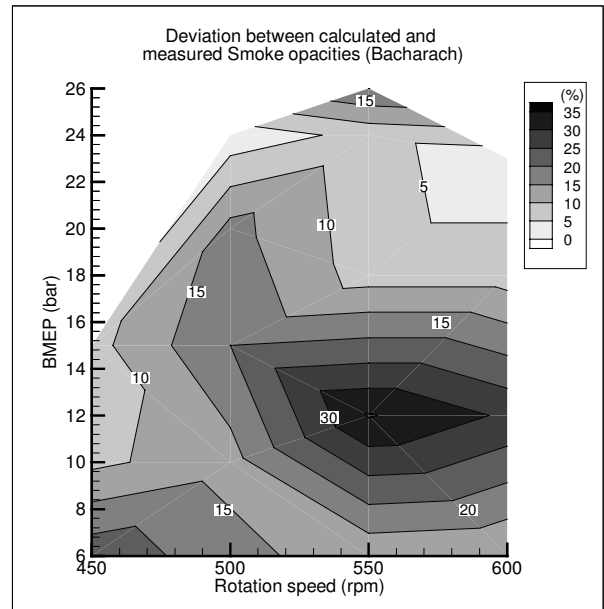


Figure 8. Difference between Measured and Simulated Smoke Opacities – Engine B

Engine A's running zones present various discontinuities due to the use of a sequential turbocharging system, especially on the boost pressure and air excess because operation can be with either one or two turbochargers. Omitting these two factors in the evaluation of the K_{TI} and Cl_{air} coefficients appears to explain the rather large difference between simulated and measured results in the area of the switch from one to two turbochargers.

Figures 7 and 8 show the difference between measured and simulated smoke opacities for each engine. The previous comments on the NOx concentrations also apply to the smoke opacities. The validation results are globally satisfactory and allow the use of the simulation code to investigate the efficiency of emission control techniques.

3. SENSITIVITY ANALYSIS FOR EMISSION CONTROL

3.1 Results

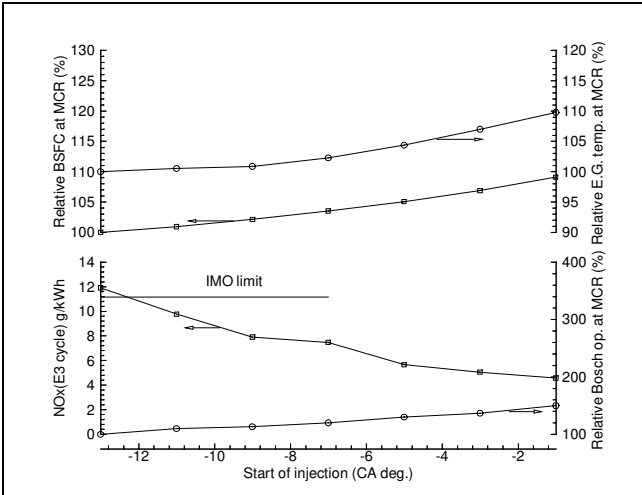


Figure 9. Influence of the Injection Timing on Pollutant Emissions and Global Engine Performance

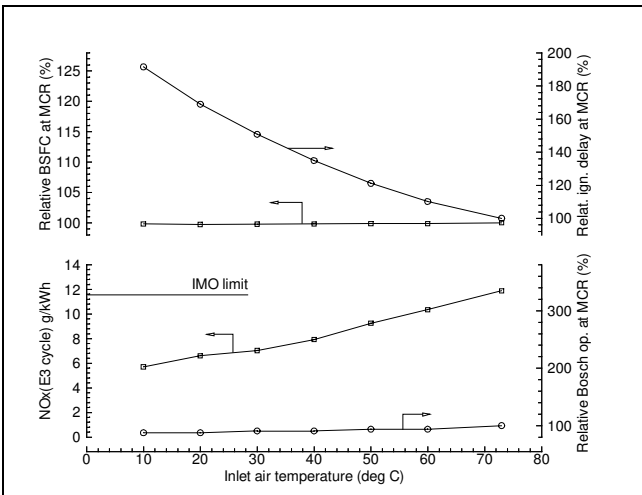


Figure 10. Influence of the Inlet Air Temperature on Pollutant Emissions and Global Engine Performance

Figure 9 through 12 show the variations of pollutant emissions and various engine performance parameters for the following techniques, respectively:

- Modification of the injection timing from 13 to 1 crank angle BTDC
- Modification of the inlet air temperature from 10 to 75 degrees Celsius
- Modification of the Exhaust Gas Recirculation (EGR) rate from 0 to 30%, as a percentage of the mass of exhaust gas added to the inlet flow

- Modification of the percentage of water added to the fuel from 0 to 60% in terms of mass quantities and in the case of a water/fuel emulsion

The results are presented for engine A. The NOx emissions are evaluated using the ISO E3 cycle that includes 4 points on the propeller curve as shown in Table 2 (ISO 1996).

Table 2. Definition of ISO E3 cycle

Mode	1	2	3	4
Speed (%)	100	91	80	63
Power (%)	100	75	50	25
Weighting factor (-)	0.2	0.5	0.15	0.15

The regulation limit is also shown on the various graphs. The smoke opacity variations are for the maximum continuous rating. In addition, the graphs show the specific fuel consumption as well as some meaningful variables such as the exhaust temperature, excess air and ignition delay. With the exception of the NOx emissions, the variations shown on the various figures are expressed with respect to a reference value of 100% corresponding to the standard engine. For example, a level of opacity of 200% is twice the level of the unmodified engine.

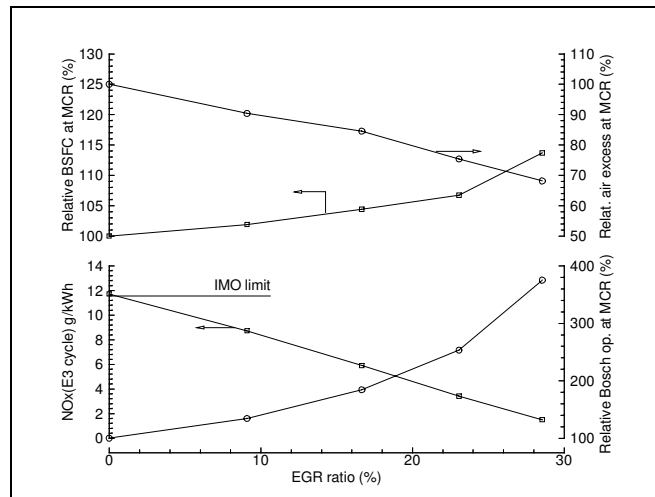


Figure 11. Influence of the EGR Rate on Pollutant Emissions and Global Engine Performance

As anticipated, all emission control techniques that were investigated lead to a significant reduction of NOx emissions, with a magnitude varying from 50% to 80% depending on the technique being used. All of them allow to easily satisfy the current requirements of the IMO regulations. Similar results were obtained quantitatively and qualitatively for engine B.

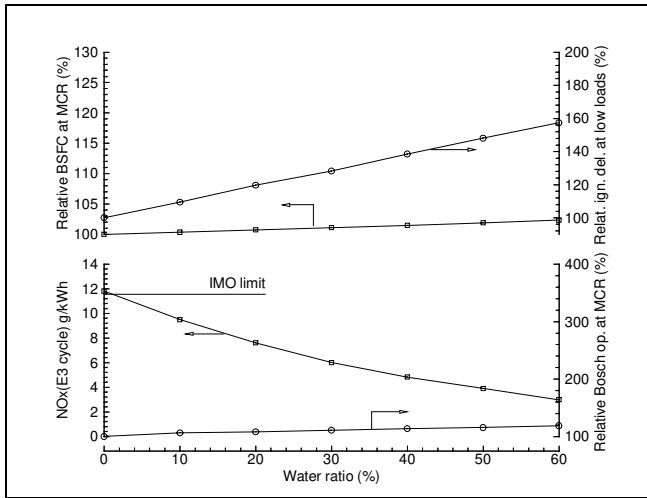


Figure 12. Influence of the Water Ratio on Pollutant Emissions and Global Engine Performance

On the contrary, the results being achieved for the reduction of smoke opacity differ depending on the technique being used. The smoke opacity seems to be barely affected by the reduction of the inlet temperature or the injection of water in emulsion whereas a significant increase occurs when reducing the injection timing, as much as 50%, and an even more significant increase is observed when recirculating the exhaust gas, as much as 300%. Again, similar results were obtained for engine B.

The simulation of emission control techniques with a complete engine model also reveals their harmful consequences on the global engine performance. The following observations were made:

- Late injection timing leads to an increase in the specific fuel consumption and may reduce the engine running range due to increased exhaust gas temperatures.
- The reduction of the inlet temperature leads to an increased severity of the combustion due to a longer ignition delay, particularly at low load.
- Exhaust gas recirculation significantly increases the specific fuel consumption and reduces excess air.
- Water injection in emulsion increases the ignition delay and also requires significant amounts of fresh water.

In addition to the issues being raised by the simulation results, some experimental studies revealed reliability problems associated with corrosion in the case of water injection as well as clogging and corrosion in the case of EGR.

3.2 Discussion

The results presented in the previous section are quantitatively in agreement with experimental results published for medium speed diesel engines, including Fleischer 1996, Murayama 1994, Remmels et al. 1995, Sonoda et al. 1995, Velji et al. 1995, Wölfe et al. 1993, and Yoshikawa et al. 1995. The reduction of NOx emissions generated by the various pollution control techniques can be explained in all cases by a decrease of the combustion gas temperature in the cylinder. Late injection timing delays the cycle

and reduces both pressure and temperature. The decrease of the inlet temperature is translated for the complete cycle. The recirculation of exhaust gas increases the gas specific heat in the cylinder and therefore limits the temperature increase induced by the compression and combustion phases. The steam produced by the injection of water in emulsion has a similar effect, although localized in the combustion zone instead of the complete cylinder.

The temperature decrease of the combustion gas is also a limiting factor for particle oxidation. A side effect is an increase of the smoke opacity. In addition, the process is amplified in the case of exhaust gas recirculation by the low oxygen content of exhaust gases, limiting the soot oxidation. On the other hand, the temperature decrease is neutralized by an increase of the air excess in the case of the inlet temperature reduction and the presence of OH molecules in the case of water injection, both factors being favorable to oxidation.

When the decrease of the cycle temperature is not compensated with another factor like a better filling ratio in the case of reduced inlet temperature, it causes a reduction of the thermodynamic efficiency, amplified by oxygen rarefaction in case of EGR, leading to an increase of the engine specific fuel consumption. In addition, the change in the combustion timing when the injection is delayed increases the gas temperature in the exhaust manifold. This can limit the engine operation range depending on materials being used, especially for the turbine. In the case of reduced inlet temperature and at a much smaller scale in the case of water injection, the ignition delay is longer due to the subsequent reduced speed of chemical reactions. Consequently, the pre-mixed combustion is more important, especially at low load, and the resulting sudden pressure increase is amplified. Getting low temperatures seem to be technically difficult.

Finally, although the efficiency of the various techniques is comparable as far as NOx emissions are concerned, their results in terms of smoke opacity and the global engine performance are very different. When selecting the appropriate technique, their individual cost must also be accounted for in terms of installation, operation and maintenance. It seems that delaying the injection process is the most interesting technique to slightly reduce the NOx emissions and meet the current IMO requirements since it is the easiest to implement. For more stringent regulations, future or local, water injection in emulsion can significantly reduce the NOx emissions (as much as 60%) while preserving the global engine performance assuming that reliability issues are thoroughly investigated. The combination of several techniques for different engine running zones can also be envisioned.

4. CONCLUSION

A multi-zone combustion model was added to the SELENDIA code to allow the evaluation of NOx emissions and smoke opacities for medium speed diesel engines. The validation that was conducted for the complete operation range of two engines representing distinct levels of powers (320 kW/cyl and 615 kW/cyl) showed a good agreement between measured and simulated data.

The code was subsequently used to investigate the efficiency of four techniques designed to reduce pollutant emissions; late

injection timing, reduction of inlet temperature, exhaust gas recirculation and water injection in emulsion. All four techniques allow a significant reduction of the NOx emissions to easily meet the IMO requirements; however, the simulation work also revealed the harmful consequences associated with each technique, particularly regarding particle emissions and global engine performance.

The enhanced code may now be used for the selection of a pollution control technique with respect to regulatory and cost constraints. In the future, further enhancements to the code will be made by using a CFD module to precisely model internal processes occurring inside the cylinder.

ACKNOWLEDGEMENTS

The authors would like to thank D.C.N. Indret (Délégation Générale pour l'Armement, France) for their financial support, and S.E.M.T. Pielstick for their technical support.

REFERENCES

- Annand W.J.D., 1963, "Heat transfer in the cylinders of reciprocating internal combustion engines" IMechE transaction
- Bazari Z. 1993, "A DI Diesel Combustion and Emission Predictive Capability for Use in Cycle Simulation" SAE 920462
- Fergusson C.R., 1986, "Internal Combustion Engines" Wiley International Edition
- Haupais A., 1982, "Modélisation phénoménologique de la combustion dans un moteur Diesel à injection Directe" Entropie No. 105
- Herrmann R., 1990, "Sequential turbocharging for PA 6 engines" ISME Kobe
- Hétet J.-F., Chessé P., Inozu B., 1994, "An ACSL simulation for optimum operation of turbocharged marine Diesel engines" Energy-sources Technology Conference-New Orleans ASME
- Hétet J.-F., Inozu B., Roy P., Tautzia X., Chessé P., 1999, "Performance Simulation of Marine Diesel Engines with SELENDIA" - Journal of Ship Research, (SNAME), Vol.43, No. 4, pp. 201-217
- Heywood J.B., 1988, "Internal Combustion Engine Fundamentals" Mc Graw Hill
- Hiroyasu H., Kadota T., Arai M., 1983, "Development and use of a spray combustion modeling to predict Diesel engine efficiency and pollutant emissions (Part 1 : Combustion Modeling and Part 2 : computational procedure and parametric study)". Bulletin of the JSME, No. 214.
- I.M.O., 1996, "Prevention of air pollution from ships (Draft)" Marine Environmental Protection Committee 39th session, 21 Novembre
- I.S.O., 1996, "Reciprocating internal combustion engines exhaust emission measurement" (Part 1: test bed measurement of gaseous and particulate emissions, Part 2: measurement of gaseous and particulate at site, Part 4: Test cycle for different engine applications) Norm ISO 8178
- Fleischer F; 1996, "NOx reduction - A technical challenge for marine Diesel engine manufacturers" International Maritime and Shipping Conference 22-24 October IMarE
- Lefebvre A.H., 1989, "Atomization and sprays" Hemisphere publishing corporation

Murayama T., 1994, "Simultaneous Reduction of NOx and Smoke of Diesel Engines without Sacrificing Thermal Efficiency" bulletin of the JSME, series B, Vol. 37, No. 1

Nishida K., Hiroyasu H., 1989, "Simplified three dimensional modeling of mixture formation and combustion in a D.I. Diesel engine" SAE 890269

Reitz R.D., Rutland C.J., 1995, "Development and testing of diesel engine CFD models" Progress in energy and combustion science Vol. 21

Remmels W., Velji A., Schmidt R.-M., Rauscher M., 1995, "An experimental and theoretical study of exhaust gas recirculation in diesel engines" C.I.M.A.C. (Interlaken)

Sonoda K., Nakano K., Yamasita H., Nakayama N., Jinja Y., 1995, "Research on improvements in Combustion of High Water-Content Emulsified Fuel" Proceedings of the ISME Yokohama Vol. I pp. 450-456

Smith W.J., Timoney D.J., 1997, "On the relative roles of fuel spray kinetic energy and engine speed in determining mixing rates in D.I. Diesel Engines" Journal of Engineering for Gas Turbines and Power. Vol. 119 pp. 212-217

Tautzia X., Hétet J.-F., Chessé P., Roy P., Inozu B., 1997, "A simulation study for medium speed Diesel engines pollutant emissions and their reduction" - ASME Fall Technical Conference of the ICE Division, proceedings Vol. 29-3, pp. 41-48, Madison Wisconsin (USA)

Tautzia X., 1998, "Simulation de l'influence des paramètres de fonctionnement des moteurs Diesel suralimentés semi-rapides sur les émissions polluantes. Etude en régime stationnaire et dynamique. Application aux ensembles utilisés en propulsion navale" - PhD Thesis - Université de Nantes et Ecole Centrale de Nantes

Velji A., Remmels W., Schmidt R.-M., 1995, "Water to reduce NO_x-Emissions in Diesel engines A basic study" C.I.M.A.C. (Interlaken)

Wofle M., Houben M., Stromberg S., Lepperhof C., 1993, "Influence of engine operating parameters on pollutant formation during diesel engine combustion" IMechE seminar Birmingham 17-18 Nov. 93

Yoshikawa S., Ogawa M., Inaba H., Fujita Y., Imamori T., Yasuma G., 1995, "The development of low NOx emission Diesel engine" C.I.M.A.C. (Interlaken)

DISCLAIMER

The contents of this paper reflect the views of the authors who are responsible for the facts and the accuracy of the data presented herein. The contents do not necessarily reflect the official views or policies of the GCRMTC or its Sites, the States of Louisiana or Texas, the U.S. Navy, or appropriate funding agency. This paper does not constitute a standard, specification, or regulation.